Accepted by *Agricultural and Forecast Meteorology*

Linking Dynamic Seasonal Climate Forecasts with Crop Simulation for Maize Yield Prediction in Semi-Arid Kenya

James W. Hansen[1]
International Research Institute for Climate Prediction
P.O. Box 1000
Palisades, NY 10964-8000
USA
+1-845-680-4410 (phone)
+1-845-680-4864 (fax)
jhansen@iri.columbia.edu (e-mail)

Matayo Indeje
International Research Institute for Climate Prediction
P.O. Box 1000
Palisades, NY 10964-8000
USA
+1-845-680-4524 (phone)
+1-845-680-4864 (fax)
mindeje@iri.columbia.edu (e-mail)

[1] Corresponding author.

Accepted by *Agricultural and Forecast Meteorology*

ABSTRACT

By providing information about growing season characteristics in advance of the season, predictions of climate fluctuations at a seasonal time scale offer opportunity to improve agricultural risk management, but only if forecasts are translated into probabilistic forecasts of production and economic outcomes of management alternatives. A mismatch between the spatial and temporal scale of dynamic climate models and process-level crop simulation models must be addressed if crop models are to contribute to the task. Methods proposed for linking crop models with dynamic seasonal climate forecasts include classification and selection of historic analogs, stochastic disaggregation, direct statistical prediction, probability-weighted historic analogs, and use of corrected daily climate model output. For a semi-arid location in Kenya, we demonstrate and evaluate methods to predict field-scale maize yields, simulated by CERES-maize with observed daily weather inputs, in response to downscaled seasonal rainfall hindcasts available prior to planting, derived from an atmospheric general circulation model, ECHAM. The methods we considered were statistical prediction by nonlinear regression, probability-weighted historic analogs and stochastic disaggregation to predict field-scale maize yields simulated by CERES-maize with observed daily weather inputs. Downscaled ECHAM output predicted 36% of the variance of total precipitation and 54% of the variance of rainfall frequency in October-December at the site. Nonlinear regression showed the lowest, and stochastic disaggregation showed the highest overall error. All of the yield forecasting methods showed similar random error, predicting from 28% to 33% of the variance of yields simulated with observed weather. Incorporating the predictability of rainfall frequency into the stochastic disaggregation procedure did not improve yield predictions. Based on this study, stochastic disaggregation, direct statistical prediction and probability-weighted historic analogs all show potential for translating seasonal climate forecasts into predictions of crop response.

Keywords: global climate models (GCM), crop simulation models, precipitation, maize, Kenya

1. INTRODUCTION

Improvements in our understanding of interactions between the atmosphere and sea and land surfaces, advances in modeling the global climate system, and substantial investment in monitoring the tropical oceans now provide a degree of predictability of climate fluctuations at a seasonal (i.e., ≥ three month) lead time in many parts of the world (Barnett et al., 1994; Palmer and Anderson, 1994; Latif et al., 1998; Goddard et al., 2001). By providing information about growing season characteristics in time to adjust strategic pre-planting management decisions, this predictability offers the potential to adjust agricultural management decisions to expected climatic variations to reduce adverse impacts or take advantage of favorable conditions.

If farmers are to apply seasonal climate forecasts to improve decision making, they must first translate forecasts into production and economic outcomes associated with alternative management strategies at the spatial scale of impacts and decisions. Locally-adapted and tested crop simulation models allow one to quickly explore the production outcomes of a range of management alternatives under a range of forecast climatic conditions (e.g., Hammer et al., 1996; Meinke et al., 1996; Carberry et al., 2000; Jones et al., 2000; Royce et al., 2001). However, the difference in spatial and temporal scales of dynamic seasonal climate prediction and crop simulation models complicate the task. Operational seasonal climate forecasts are typically expressed as climatic anomalies or tercile probability shifts averaged in space at the scale of GCM (general circulation model) grid cells (currently on the order of 10,000 km^2), and averaged in time over three-month seasons. This convention maximizes prediction skill by reducing the "noise" associated with weather variability in time and space that can mask predictable seasonal climatic variations. Near the other end of the time-space continuum, dynamic, process-oriented crop simulation models typically assume a spatially-homogeneous environment (i.e., a single plot). These models are designed to capture the dynamic, nonlinear interactions between weather, soil water and nutrient dynamics, management, and the physiology and phenology of the crop, typically on a daily time step. Crop production and appropriate management decisions may depend more on the distribution of rainfall within a season than on the

season averages that forecasters typically provide. The time of growing season onset, probability of water deficit during critical periods for yield determination, and conditions during ripening, harvest and drying are among the important determinants of crop production.

Although dynamic climate models operate on sub-daily time steps and can therefore generate daily sequences of meteorological variables, the spatial averaging that occurs within grid cells distorts the temporal variability of daily weather sequences (e.g., Mearns et al., 1995; Goddard et al., 2001). Because of the many nonlinear processes that they embody, any biases in variability of daily weather can seriously distort crop model prediction (Semenov and Porter, 1995; Mearns et al., 1996; Riha et al., 1996; Mavromatis and Jones, 1998; Hansen and Jones, 2000). This is particularly important for precipitation because of its influence on processes, such as solute leaching, soil erosion and crop water stress response, that depend on soil water balance dynamics. Dynamic climate models tend to produce too many rainfall events, with too little rain per event. This distortion can result in either under-prediction of crop yields due to increased evaporative loss from the soil surface, or over-prediction due to reduced dry spell duration (de Wit and van Keulen, 1987; Carbone, 1993; Mearns et al., 1996; Riha et al., 1996).

The spatio-temporal scale mismatch between dynamic climate models and crop simulation models presents a substantial challenge to using crop simulation to anticipate crop response to predicted climate variations. Extracting and applying information about within-season variability for crop model applications remains a more difficult challenge than downscaling in space. Several approaches for linking crop simulation models with seasonal climate forecasts have been proposed.

In this paper, we provide an overview of some of these methods, and demonstrate and evaluate a subset of these methods – statistical prediction by nonlinear regression, probability-weighted historic analogs and stochastic disaggregation – for predicting field-scale yield response to downscaled rainfall hindcasts derived from an atmospheric general circulation model (GCM). As a test case, we consider simulated maize under conditions at the Katumani Dryland Research Station (1° 35' S, 37° 14' E, 1601 m.a.s.l.) in the Machakos District of eastern Kenya. Maize in this region depends on rainfall in the October-December short rain season associated with the southward propagation of the inter-tropical convergence zone. We selected the site for several reasons. A large segment of the population in the region depends on rainfed maize for subsistence. Maize production is risky in this semi-arid environment due in part to its sensitivity to year-to-year variability in the amount and timing of rainfall. However, predictability of the short rains at a seasonal time scale is quite high over the portion of Kenya that encompasses the study site (Fig. 1). Rainfall in this region is strongly linked to the El Niño-Southern Oscillation (ENSO) (Ropelewski and Halpert, 1987, Ogallo et al., 1988, Indeje et al., 2000, Mutai et al., 1998). The Machakos District was the focus of a survey of 240 farm households (Ngugi, 2002) that revealed widespread awareness of seasonal climate forecasts, opportunities for modifying crop management in response to forecasts, and strong interest in expanding use of forecasts. Our study benefits from previous model-based research at the Katumani site (Probert, 1992, Keating et al., 1993). Due to lack of availability of observed crop yield time series and associated data sets, our evaluation focuses on using GCM-based seasonal climate predictors with a crop simulation model to predict yields simulated observed daily weather, and not on the crop model's ability to simulate observed yields.

2. Approaches for Linking Seasonal Climate Predictors and Crop Models

Figure 2 shows a set of plausible information pathways from large-scale climatic forcing to simulation-based crop yield prediction. Yield prediction can be based on either (*a*) simulation using daily time series data that are somehow conditioned on the forecast, or (*b*) a statistical model of crop yields as a function of some climatic predictor variables. For pathway (*a*), daily weather inputs can come directly from the daily output of a dynamic atmospheric general circulation model (GCM) or high-resolution regional climate model (RCM) nested within GCM output fields (*c*), downscaled to the local scale. An alternative to using daily climate model output

is to use lower-frequency (e.g., monthly or seasonal) predictions, then apply a disaggregation process to produce realizations of daily weather as input to the crop model, using, e.g., a stochastic weather generator (*d*). The same disaggregation procedure is applicable to statistical seasonal climate forecasts (*e*). Pathway (*b*) predicts yields as a statistical function of either observed climate predictors (*f*) or dynamic climate model output fields (*g*), trained on time series of crop yields simulated using observed daily station data (*h*). Finally, what has been the "standard approach" for some time (*i*) is to categorize the observed predictor variables (e.g., ENSO phases), and use the predictor category to select sets of analog years from the observed station time series as input to the crop model. These potential information pathways suggest several potential approaches for linking dynamic crop simulation models with climate predictors via dynamic climate models.

Classification and selection of historic analogs. The most common approach to using seasonal forecasts with agricultural models has been to divide the range of variability of climatic predictors into a small set of categories or "phases" based on some objective criterion (e.g., Trenberth, 1997), then select the set of past years falling within a given category as equally-probable analogs (pathway *i*, Fig. 2). Historic analogs are easily interpreted at any spatial and temporal scale for which data are available, and provide daily weather series at individual stations for driving crop simulation models. Distributions of climatic realizations or simulated production or economic outcomes for the set of analog years associated with a given category provide an intuitive probabilistic interpretation. To-date, most efforts to predict crop response at a seasonal time scale, and most quantitative studies of agricultural decisions tailored to seasonal climate forecasts have used this approach with categorical indices based on sea surface temperatures or the Southern Oscillation Index (SOI), both associated with ENSO. Although analogs are usually derived from observed climatic predictors, Stone et al. (2000) proposed using cluster analysis to categorize GCM output fields as a basis for selecting analog years for use with crop simulation, and illustrated the approach over eastern Australia.

Stochastic disaggregation. A second approach to linking climate prediction to agricultural models is to aggregate bias-corrected climate model output into seasonal or sub-seasonal (e.g., monthly) averages, then disaggregate to produce daily time series with high-frequency variability that is consistent with the long-term daily record, and low-frequency variations that represents the seasonal or sub-seasonal forecasts (pathways *d* and *e*, Fig. 2). Temporal disaggregation involves the use of some form of stochastic weather generator. Two approaches have been advanced. The first is to condition the parameters of a stochastic generator on a given forecast (e.g., Briggs and Wilks, 1996; Wilks, 2002) or set of climatic predictors (e.g., ENSO phases, Woolhiser et al., 1993; Grondona et al., 2000). The second approach, which we apply in this study, is to constrain the generated daily sequences to match predicted monthly or seasonal means and other statistical properties.

Direct statistical prediction. One can condition the output rather than the inputs of a crop model on climatic predictor variables (pathway *b*, Fig. 2), thereby avoiding the need for daily weather sequences conditioned on a given forecast. The underlying assumption is that large-scale seasonal predictors of local-scale meteorological determinants of crop yields (e.g., precipitation, temperatures) are also potential statistical predictors of crop yields. Annual time series of crop response simulated with observed daily weather can serve as the predictand. Use of regression must consider the tendency for most crops to show non-linear and sometimes non-monotonic relationships to varying seasonal rainfall totals. Although it is intuitively attractive, this approach has not yet been widely tested or exploited.

Probability-weighted historic analogs. A variant of both historic analogs and regression derives probabilistic crop forecasts from probability-weighted historic analogs. In the absence of a skillful forecast, we typically use the historic distribution to predict the coming season, assigning equal probability to all past years. If we have a basis for predicting that the coming season is more likely to resemble some past years than others, we can use the shifted probability weights to derive a shifted distribution, or calculate distribution statistics, of simulated crop response. Several operational forecast centers express seasonal forecasts as probability shifts from historic climatic tercile categories (e.g., Mason et al., 1999). The *k*-nearest neighbor approach (Lall and Sharma, 1996) selects and weights a subset of a predictand (e.g., crop yields simulated with observed weather) time series according to the degree of similarity, based on the vector of predictors (e.g., observed SSTs or GCM output), to the current state of

predictors. This approach can be interpreted as either an analog approach (pathway *i*, Fig. 2) or as a semi-parametric local regression model (pathway *b*, Fig. 2).

Finally, we can consider *direct use of daily dynamic climate model output* (pathway *c*, Fig. 2). However, as discussed earlier, dynamic climate models tend to distort the temporal variability of their daily output, with serious consequences for crop simulation. However, more sophisticated handling of daily climate model output, such as separate estimation of rainfall occurrence and intensity and the addition of stochastic variability (Wilby et al., 2002), has the potential to reduce the resulting errors.

3. METHODS

3.1. GCM Predictor Selection and Rainfall Hindcasts

We used climate forecast fields from the GCM, ECHAM v.4.5 (Roeckner et al., 1996), developed at the Max-Plank institute (Germany). ECHAM was run for 1961-1999 at a T42 (approximately 2.8°) horizontal resolution, with 18 vertical levels. We used output from simulations that the International Research Institute for Climate Prediction (http://iri.columbia.edu) previously ran as input to their operational seasonal forecasts. We analyzed the mean of an ensemble of twenty-four GCM integrations, each run with different initial atmospheric conditions sampled each year from global observations on different days of the forecast month, but the same sea surface temperature (SST) boundary conditions. Although the output of ECHAM simulated with concurrent observed SSTs served the purpose of the present methodological comparison study, the results likely overstate the predictability obtainable under operational conditions where forecast SSTs must be used for any future prediction period (Goddard and Mason, 2002). We used GCM output that, in an operational mode could be available by the first of October to predict October-January rainfall.

The coarse spatial resolution of current GCMs often lead to systematic shifts in the location of spatial rainfall patterns that reduce their prediction skill. Since the large-scale features that the GCM can predict affect local seasonal climate variations, it is possible to use this information to improve prediction of local climate variability (Benestad, 2001). Model correction is necessary to account for shifts in regional rainfall anomaly patterns that results from the influence of local factors that the coarse resolution of GCMs cannot capture, such as, steep orography, vegetation contrasts and land-water contrasts. The use of statistical relationships, estimated over some past period, between observed climatic predictand fields and hindcast GCM output fields, is known as model output statistics (MOS) (Zorita and von Storch, 1999; Solman and Nuñez, 1999). When the predictand is at a higher spatial resolution than the GCM output, the approach is known as MOS downscaling, or statistical downscaling. One common approach to MOS correction or downscaling uses principal component analysis applied to identify the leading modes of variability of the GCM output fields, and sometimes the predictand spatial fields (Heyen et al., 1996; Kidson and Thompson, 1998). Each principal component (PC) pattern represents a predictor field with high spatial resolution and spatial coherence, yet without the risk of over-fitting the empirical model. These can then be related to the predictands by regression. Comparison between the PC modes of the observations and GCM simulations allows simple model evaluation (Feddersen et al., 1999; Benestad, 2001).

To select optimum predictor GCM fields, we tested a combination of rainfall and low-level circulation fields in isolation and in combination. We used the GCM precipitation spatial field alone, as the combination of the two-predictor fields did not significantly increase forecast skill. The geographical domain for our MOS correction was bounded by 6°N to 6°S and longitudes 33°E to 43°E. The predictand field was precipitation (seasonal and monthly) from 52 stations covering Kenya and the surrounding countries. The first two leading principal component time series (*PC1* and *PC2*) chosen explained 59 and 15% of the variance of the observed seasonal rainfall spatial field. The MOS correction resulted in high prediction skill (r>0.7 for 1961-1999) over most of the region.

At the Katumani site, October-December rainfall and both PCs showed positive skewness. Scatter plots (Fig. 3) do not show evidence of a nonlinear relationship between rainfall and either PC. A *t*-test confirmed a lack of influence of *PC2* on rainfall that is apparent in

the scatter plot. We therefore predicted October-December rainfall total as a linear function of only *PC1*. Leave-one-out cross-validation ensured that observations from the forecast period did not directly influence forecasts, while allowing us to make efficient use of limited data (Stone, 1974). For each year i, we solved the model by least-squares regression using simulated yields and *PC1* from each year $j \neq i$, then calculated $\hat{y}$ from the fitted slope and intercept and *PC1* for year i. We generated and evaluated hindcasts of rainfall totals in individual months, and relative rainfall frequency and mean wet-day intensity by cross-validated linear regression from *PC1* in the same manner.

3.2. Climate Data

The Katumani Dryland Research Station is a government research station with international support. It routinely measures climate data (i.e., rainfall, temperature, sun shine hours, humidity). We used daily rainfall observations from 1961-1999 based on the availability of both rainfall observations and output of ECHAM hindcast runs. We omitted the 1990, 1991 and 1995 crop seasons from analyses because they had substantial gaps of precipitation observations. We derived seasonal and monthly rainfall totals, frequencies and mean intensities from the daily observations.

Measured temperatures were available only since 1984, and solar irradiance only for January 1986 to September 1998. B.A. Keating graciously provided daily estimates of missing daily minimum and maximum temperature and solar irradiance through 1988, based on regression relationships fit for the period of available data and conditioned on rainfall occurrence, as described in Probert et al., 2001. For the remainder of the period, synthetic series of these variables derived from a stochastic weather generator and conditioned on rainfall occurrence (Pickering et al., 1994) were used as a proxy for observations.

3.3. Crop Simulation

Yields of maize were simulated by CERES-Maize v. 3.5 (Ritchie et al., 1998). Required model inputs include daily weather data (minimum and maximum temperature, precipitation and solar irradiance), soil properties, initial soil water content, cultivar characteristics, planting date and spatial arrangement, and N fertilizer management. Soil properties, characteristics of the short-season cultivar, 'Katumani,' composite B, and representative management assumptions were based on a previous study at the same site (Keating et al., 1992). For each simulation year, the water balance was initialized on October 1 with soil water at 20% of capacity. Planting was simulated the first time, within an October 1 to November 1 planting window, that water content reached at least 40% of capacity averaged through the top 15 cm. Planting was forced on November 1 if conditions were not reached within the planting window. We assumed application of 20 kg N ha^{-1} as ammonium nitrate at planting, based on economic analyses presented by Probert et al. (1994). Stand density was 4.4 plants m^{-2}, with a 50 cm inter-row spacing.

3.4. Maize Hindcast Scenarios

We tested six maize prediction scenarios (Table 1), run in a hindcast mode, for their ability to predict maize yields simulated in a baseline scenario with observed daily weather as described in the previous section. Evaluating predictability in a hindcast mode requires that (a) initial conditions (e.g., soil water contents) are consistent across scenarios, (b) antecedent boundary conditions (e.g., weather inputs) represent observations from the hindcast year, and (c) observations from the period being forecast do not influence forecasts. To simplify analyses and interpretation, we avoided the need to run simulations with antecedent weather data for each year by initializing the soil profile and starting the water balance on the first day of the forecast period. Yet we recognize that either initializing the water balance with observed soil water contents or simulating the water balance with antecedent weather data prior to the start of the forecast period can improve prediction. Consistent use of cross-validation ensured that observations from the forecast period did not directly influence the forecasts.

3.4.1. Regression from climate predictors

Simulated maize responds non-linearly and non-monotonically to seasonal rainfall (Fig. 3). The relationship of *PC1* to simulated yields also appear to be nonlinear. A Mitscherlich function,

$$\hat{y} = a + b\left(1 - \exp\left(-c\,x\right)\right) \qquad (1)$$

and its variants are often used to predict crop yield, y, as a function of water available through the growing

season, x (e.g., Vaux and Pruitt, 1983). The Mitscherlich function assumes that yields approach their maximum, a, asymptotically in proportion to the distance from the maximum, as a function of increasing supply of some essential growth factor x. Because the relationship between seasonal rainfall and *PC1* is approximately linear, we applied Eq. 1 to predict yield as a function of *PC1*. We applied the nonlinear regression in a cross-validated mode in the same manner as described earlier for rainfall hindcasts by linear regression.

3.4.2. *k* nearest neighbor weighted analogs

The *k*-nearest neighbor (knn) method selects and assigns probability weights to a subset of *k* analog years based on their rank Euclidian distance, in predictor state space, to a given predictor state (Lall and Sharma, 1996) . The expected value of predictand y in year t of a series is estimated as a weighted average of yields simulated using yields from the k analog years:

$$\hat{y}_t = \sum_{i=1, i \neq t}^{n} w_i y_i \qquad (2)$$

Weights w of the k nearest neighbors are based on their rank distance to the value of the predictor vector:

$$w_j = \frac{1/j}{\sum_{i=1}^{k} 1/i} \qquad (3)$$

where i is the index of the neighbor, sorted by distance (closest to furthest) from the predictor vector. For all $i > k$, w_i is set to 0.

We applied the knn method using *PC1* alone, and using both predictors. The knn method can be regarded as a nonlinear, semi-parametric local regression method. Although *PC2* did not contribute significantly to predictability October-December rainfall using a global linear regression model, we included it in a second knn scenario based on the possibility of a local influence on the meteorological determinants of simulated maize yields over some part of the range of variability. To account for the relative influence of the two GCM predictors, we re-scaled *PC1* and *PC2* by multiplying each by its coefficient of linear multiple regression, β_{PC1} and β_{PC2} obtained from least-squares regression of $\hat{y} = \alpha + \beta_{PC1} PC1 + \beta_{PC2} PC2$. We selected the number of neighbors, k, that minimized cross-validated *RMSE*.

3.4.3. Stochastic disaggregation of monthly precipitation

We used a stochastic weather generator that is modified to allow it to generate synthetic daily weather sequences such that the monthly climatic means exactly match specified targets. The underlying stochastic generator is described in Hansen and Mavromatis (2001). It is an adaptation of the WGEN weather generator of Richardson (1985). Enhancements include an improved stochastic solar irradiance component (Hansen, 1999), a hybrid-order Markov chain for precipitation occurrence (Stern and Coe, 1984), a hyperexponental distribution of precipitation intensity (Woolhiser and Roldán, 1982), and partitioning of variability of temperatures and solar irradiance into high- and low-frequency components.

The total amount of rainfall in a given month is a function of both the frequency of rainfall occurrence and the distribution of amounts on days with rain (i.e., intensity). Total rainfall tends to be positively correlated with both frequency of wet days and mean intensity on wet days. (For October-December rainfall at Katumani, r=0.737 for frequency and r=0.684 for intensity.) Adjusting generated daily rainfall by a constant multiplier to match a target could produce unrealistic combinations of rainfall frequencies and intensities if the monthly target is much different from the generated amount. To avoid unrealistic frequency-intensity combinations, rainfall for a given month m is stochastically generated repeatedly until the mean daily amount $\overline{R}_m$ is within 5% of the target R_m^*. The daily series generated for the month is then rescaled by multiplying R_j for each day j by $R_m^* / \overline{R}_m$. The approach we used is designed to preserve the historic consistency between occurrence and intensity of rainfall, on the assumption that GCM-based climate forecasts provide no useful information beyond monthly rainfall totals.

We applied stochastic disaggregation within two scenarios (Table 1). First, for each hindcast year we generated 30 stochastic realizations of daily weather whose monthly totals match October to January monthly

totals predicted from *PC1*. Using monthly GCM output fields, we applied the same statistical transformation and cross-validated regression procedure described earlier for seasonal rainfall totals, to generate hindcasts of each month's rainfall. The linear procedure results in monthly rainfall totals whose sums follow the hindcast seasonal totals closely. Because the seasonal GCM predictions are considered more accurate than monthly predictions, we applied a multiplicative adjustment to October, November and December hindcast rainfall totals to make them exactly match the October-December seasonal hindcasts.

The second stochastic disaggregation scenario incorporated hindcasts of monthly rainfall frequency into the stochastic generation procedure. Rainfall frequency showed good predictability from *PC1* in the months of October-December (Table 2), providing additional information about the distribution of rainfall within the season. Rainfall intensity was not significantly associated with the GCM predictor. We generated thirty stochastic realizations of daily weather whose monthly totals matched October-January hindcasts, followed by adjustment for October-December totals, as we did for the first scenario. However, we replaced the rainfall occurrence Markov transition probabilities calculated from the long term record with transition probabilities based on each year's predicted probability of occurrence, π, for October-December. This scenario therefore incorporates the predictable components of total monthly rainfall and rainfall frequency.

The use of a hybrid second-order Markov chain better represents distribution of dry spells than the geometric distribution embodied in a first-order model (Stern and Coe, 1984; Wilks, 1999), but complicates the adjustment of Markov transition probabilities somewhat. The procedure, described in Hansen and Mavromatis (2001) in the context of a low-frequency variability bias correction, involves adjusting three unique transition probabilities, p_{11}, p_{001} and p_{101}, in a manner that represents predicted π but preserves first- and second-order persistence, ρ_1 and ρ_2, of the Markov process. Briefly, for a given calendar month let

$$q_{ij} = \mathbf{P}\left\{s_{t-1} = i, s_t = j\right\} = \pi_i p_{ij} \tag{4}$$

define the probability of an i, j sequence, where $\pi_1 \equiv \pi$ and $\pi_0 \equiv 1 - \pi$, and s_t represents rainfall occurrence (s=1) or non-occurrence (s=0). Let π_y' denote π (probability of rainfall occurring on a given day) predicted for year y, and p_{ij}' and p_{ijk}' denote adjusted transition probabilities. First- and second-order persistence of dry days are given by

$$\rho_1 = p_{11} - p_{01} \tag{5}$$

and

$$\rho_2 = p_{101} - p_{001} \tag{6}$$

Then the adjusted transition probabilities are obtained from,

$$p_{01}' = \pi'\left(1 - \rho_1\right) \tag{7}$$

$$q_{01} = p'\left(1 - \pi'\right) \tag{8}$$

$$q_{00} = 1 - \pi' - q_{10} \tag{9}$$

$$p_{11}' = p_{01}' + \rho_1 \tag{10}$$

$$p_{001}' = \frac{q_{01}' - q_{10}'\rho_2}{q_{00}' + q_{10}'} \tag{11}$$

$$p_{101}' = p_{001}' + \rho_2 \tag{12}$$

3.5. Analyses

We use standard descriptive measures of goodness-of-fit to evaluate predictability of both rainfall and simulated yield hindcasts. Mean-squared error of prediction, or prediction variance,

$$MSE = n^{-1}\sum_{t=1}^{n}\left(\hat{y}_t - y_t\right)^2 \tag{13}$$

represents overall error weighted by the square of deviations, where n is number of years t, y and $\hat{y}$ are observed and predicted values. After Willmott (1982), *MSE* can be decomposed into a random component that is not correctable by a linear transformation,

$$MSE_R = n^{-1}\sum_{t=1}^{n}\left(\hat{y}^*_t - y_t\right)^2 \quad (14)$$

and a systematic component that can be corrected by linear regression,

$$MSE_S = MSE - MSE_R \quad (15)$$

where $\hat{y}^*$ is $\hat{y}$ calibrated by linear regression. The square root of equations 13-15, *RMSE*, $RMSE_R$ and $RMSE_S$, express error in units of the predictand variable, but are not additive. We also consider Pearson's coefficient of linear correlation, *r*, mean bias error,

$$MBE = n^{-1}\sum\left(\hat{y}_t - y_t\right) \quad (16)$$

and the index of agreement,

$$d = 1 - \left[\sum_{t=1}^{n}\left(\hat{y}_t - y_t\right)^2 \Big/ \sum_{t=1}^{n}\left(\left|\left(\hat{y}_t - \bar{y}\right)\right| + \left|\left(y_t - \bar{y}\right)\right|\right)^2\right] \quad (17)$$

Willmott (1981, 1982) proposed *d* as a 0-1 unitless measure of model agreement that accounts for both systematic and random error.

4. Results and Discussion

4.1. Predicted Seasonal Precipitation

Residuals of October-December total rainfall and relative frequency as linear functions of *PC1* (not shown) showed no apparent systematic shifts of mean or variance as a function of the predictor. However, the residuals of total rainfall deviated significantly from a normal distribution (Shapiro-Wilk W=0.816, p<0.0001), showing significant positive skewness (g_1 = 1.77). Residuals of mean relative frequency showed marginal evidence of non-normality (Shapiro-Wilk W=0.939, p=0.052) associated with negative skewness (g_1 = -0.75).

Based on cross-validated linear regression from *PC1*, the ECHAM model predicted about 36% of the variance of October-December rainfall (Fig. 4a, Table 2). Predictability of total rainfall for individual months was significant in October, November and December, and highest in November (Table 2). Mean rainfall frequency showed higher predictability than the total quantity of rainfall in the October-December period (Fig. 4b). Under cross-validation, ECHAM predictors explained about 54% of the observed variance (based on r^2, Table 2). Like total rainfall, monthly rainfall frequency showed significant predictability for October, November and December, with predictability highest in November. Cross-validated ECHAM-based hindcasts of mean rainfall intensity on wet days were not significantly correlated with observed mean intensities (Fig. 4c).

4.2. Predicted Maize Yields

Figures 5 and 6 and Table 3 summarize results of the various maize yield hindcast scenarios. Nonlinear regression showed the lowest overall prediction error, followed by the two knn scenarios, then stochastic disaggregation. Regression and knn showed negligible systematic error. However, the stochastic disaggregation scenarios both showed substantial positive mean bias, resulting in substantially higher $RMSE_S$ than the other methods. Random error – the component that is not correctable by linear calibration – differed surprising little among the five hindcast methods. The five methods predicted from 28% (knn, 1 PC) to 33% (stochastic disaggregation) of the variance of yields simulated with observed weather. Random error was lowest from stochastic disaggregation based only on monthly rainfall totals, and from nonlinear regression.

Figure 7a shows the least-squares curve (Eq. 1) trained on the full set of yields and *PC1*. We evaluated residuals (Fig. 7b) for possible violations of the assumptions of least-squares nonlinear regression. The Shapiro-Wilk test (W=0.950, p=0.111) did not indicate significant departure from normality. To test for systematic departures from homogeneity of variances, we split the residuals, sorted by the independent variable (*PC1*), and applied the Brown-Forsythe (1974) test to the first 17 vs. the second 18 residuals. Results of the Brown-Forsythe

test were marginal (p=0.065), indicating that variability of residuals may decrease systematically with increasing *PC1*. This may result in part from the relatively low density of observations at high values of *PC1*, which allows the flexible function to follow the observations more closely than at low values of *PC1*, where observations are more clustered. We do not consider this marginal departure from homogeneity of variances to be sufficient to invalidate the nonlinear regression model.

Figure 8 shows the sensitivity of yield predictions to the number of neighbors, *k*, when both PCs were used. Prediction error (*RMSE*) decreased sharply as *k* increased from 1 to 8, then reached a minimum at 15. Prediction goodness-of-fit statistics were fairly insensitive to values of *k* above about 12. The optimal number of neighbors was considerably higher in this case than the $k = \sqrt{n}$ rule-of-thumb that Lall and Sharma (1996) proposed. Bias of mean and variance and low correlation contributed to high prediction error at low values of *k*. Variations of errors as a function of *k* was roughly similar for the scenario that only used *PC1*, which also had an optimal *k* of 15. Results in Table 3 and Fig. 5b, c and 6 are based on *k*=15.

Contrary to expectation, incorporating the predictability of rainfall frequency into the stochastic disaggregation process did not improve prediction of simulated maize yields, and increased prediction error slightly. The reason for the increase in error is not apparent. The source of the positive mean bias observed with stochastic disaggregation is also not obvious. We can speculate that it may be based on the highly nonlinear maize yield response to rainfall, and under-representation of rainfall variability in the deterministic procedure we used for predicting monthly rainfall totals from GCM output. Hindcasts produced by linear regression tends to exhibit lower variability than the observed data used to fit the regression model. When crop response to a varying input is concave with increasing amount, any reduction in the variability of that input into a predictive model will tend to result in positive mean prediction bias (Hansen and Jones, 2000). Another possibility is that the weather generator used in the stochastic disaggregation process may under-represent long dry spells. However, tests with other crop scenarios did not show any tendency for synthetic weather to result in yield over-prediction (Hansen and Mavromatis, 2001; Mavromatis and Hansen, 2001).

5. CONCLUSIONS

Results demonstrate that feasible options exist for linking large-scale seasonal rainfall forecasts derived from GCMs with crop simulation for yield forecasting. However, they do not identify any one method as clearly superior. After correcting for systematic error, regression, knn resampling and stochastic disaggregation provide comparable predictability. Based on the results, regression and knn may be preferred over stochastic disaggregation due to the mean bias and the relative complexity of stochastic disaggregation. There is a clear need to evaluate the range of methods across a range of climates, sites, crops, soils and management scenarios before recommending particular methods for forecasting crop response using GCM-based seasonal climate forecasts for particular applications.

As expected (e.g., Barrett, 1998), our results showed lower predictability for simulated yields than for seasonal rainfall totals. Yet the difference in predictability of rainfall and yields, as indicated by *r* or *d* (Tables 2, 3), was rather small. Cane et al. (1994) showed that statistical association with ENSO-related sea surface temperatures in the NINO3 (90°-150°W, 5°S-5°N) region of the Pacific was greater for country-average maize yields (1970-1993) in Zimbabwe than for country average rainfall. Rosenzweig (1994) suggested that ENSO may provide predictive information about characteristics of rainfall variability that influence Zimbabwe maize yields beyond season total rainfall, and that may be discarded by averaging through the season. Our use of monthly rather than seasonal predictions for stochastic disaggregation may have incorporated some information about the distribution of rainfall within the season. The other methods (regression and knn) incorporate any predictability of higher-order statistics embodied in the GCM predictors, into the statistical transfer functions. However, contrary to our expectation, explicitly incorporating the predictability of π into the stochastic disaggregation procedure failed to improve yield forecasts.

The degree to which the predictability of regional rainfall response to large-scale SST forcing translated into predictability of crop yields is cause for optimism. It suggests that crop simulation can be used to explore management responses to GCM-based seasonal climate forecasts that might improve farmer livelihoods. Scaling up crop model-based yield forecasts to a regional scale (Hansen and Jones, 2000) might provide useful information for food insecurity early warning. Any decision application must consider that empowering smallholder farmers to benefit from seasonal climate forecasts through improved crop management requires much more than predicting yield impacts. Specific limitations of this study should also be considered prior to any decision applications. First, to avoid false skill from using concurrent SSTs, GCM hindcasts based on predicted or persisted SSTs should be used to give a conservative estimate of predictability of rainfall. Second, because the predictand was simulated and not measured yields, the results do not provide an accurate measure of maize yield predictability. Actual prediction error is likely to be substantially greater than the results of our analyses, and will be highly dependent on accurate input data, the availability and quality of data for calibration and evaluation, the particular determinants of yields at the site, and the skill of the analyst. We expect that maize yield prediction can be improved further by, e.g., initializing the soil profile with measured water contents or initializing the water balance earlier using antecedent rainfall.

ACKNOWLEDGMENTS

We gratefully acknowledge helpful discussion with U. Lall, and M.N. Ward. B. Keating provided soil .and early weather data. This work was supported by a grant/cooperative agreement number NA67GP0299 from the National Oceanic and Atmospheric Administration. The views expressed herein are those of the author and do not necessarily reflect the views of NOAA or any of its sub-agencies.

REFERENCES

Barnett, T.P., Beingtsson, L., Arpe, K., Flügel, M., Graham, N., Latif, M., Ritchie, J., Roeckner, E., Schlese, U., Schulzweida, U., Tyree, .M., 1994. Forecasting global ENSO-related climate anomalies. Tellus 46A, 381-397.

Barrett, C.B., 1998. The value of imperfect ENSO forecast information: discussion. Am. J. Agric. Econ. 80, 1109-1112.

Benestad, R.E., 2001. A comparison between two empirical downscaling strategies. Int. J. Climatology 21, 1645-1668.

Briggs, W.M., Wilks, D., 1996. Extension of the CPC long-lead temperature and precipitation outlooks to general weather statistics. J. Climate 9, 3496-3504.

Brown, M.B., Forsythe, A.B., 1974. Robust tests for the equality of variances. J. Amer. Statistical Assoc. 69, 264-267.

Cane, M.A. Eshel, G. Buckland, R.W., 1994. Forecasting Zimbabwean maize yield using eastern equatorial Pacific sea surface temperature. Nature 371, 204-205.

Carberry, P., Hammer, G.L., Meinke, H., Bange, M., 2000. The potential value of seasonal climate forecasting in managing cropping systems. In: Hammer, G.L., Nicholls, N., Mitchell, C. (Eds.), Applications of Seasonal Climate Forecasting Agricultural and Natural Ecosystems. Kluwer, Dordrecht, The Netherlands, pp. 167-181.

Carbone, G.J., 1993. Considerations of meteorological time series in estimating regional-scale crop yield. J. Climate 6, 1607-1615.

de Wit, C.T. van Keulen, H., 1987. Modelling production of field crops and its requirements. Geoderma 40, 253-265.

Fedderson, H., Navarra, A., Ward, M.N., 1999. Reduction of model systematic error by statistical correction for dynamical seasonal predictions. J. Climate, 12, 1974-1989.

Goddard, L., Mason, S.J., 2002. Sensitivity of seasonal climate forecasts to persisted SST anomalies. Climate Dynamics 19, 619-632.

Goddard, L., Mason, S.J., Zebiak, S.E., Ropelewski, C.F., Basher, R., Cane, M.A., 2001. Current Approaches to Seasonal to Interannual Climate Predictions. Int. J. Climatology 21, 1111-1152.

Grondona, M.O., Podestá, G.P., Bidegain, M.,Marino, M., Hordij, H., 2000. A stochastic precipitation generator conditioned on ENSO phase: A case study in southeastern South America. J. Climate 13, 2973-2986.

Hammer, G.L., Holzworth, D.P., Stone, R., 1996. The value of skill in seasonal climate forecasting to wheat crop management in a region with high climate variability. Australian Journal of

Agricultural Research 47, 717-73.
Hansen, J.W., 1999. Stochastic daily solar irradiance for biological modeling application. Agric. For. Meteorol. 94, 53-63.
Hansen, J.W., Jones, J.W., 2000. Scaling-up crop models for climate variability applications. Agric. Systems 65, 43-72.
Hansen, J.W., Mavromatis, T., 2001. Correcting low-frequency bias in stochastic weather generators. Agric. For. Meteorol. 109, 297-310.
Heyen, H., Zorita, E., von Storch H., 1996. Statistical downscaling of monthly mean North Atlantic air-pressure to sea level anomalies in the Baltic Sea. Tellus, 48A: 312-323.
Indeje, M., Semazzi, F.H.M., Ogallo, L.J., 2000. ENSO signals in East African rainfall and their prediction potentials. Int. J. Climatol. 20, 19-46.
Jones, J.W., Hansen, J.W., Royce, F.S., Messina, C.D., 2000b. Potential benefits of climate forecasting to agriculture. Agriculture, Ecosystems and Environment 82, 169-184.
Keating, B.A., Wafula, B.M., Watiki, J.M., 1992. Exploring strategies for increased productivity – the case for maize in semi-arid Eastern Kenya. In: Probert, M.E. (Ed.), A Search for Strategies for Sustainable Dryland Cropping in Semi-arid Eastern Kenya. ACIAR Proceedings No. 41. Australian Centre for International Agricultural Research, Canberra, Australia, pp. 90-101.
Keating, B.A., McCown, R.L., Wafula, B.M., 1993. Adjustment of nitrogen inputs in response to a seasonal forecast in a region of high climatic risk. In: Penning de Vries, F.W.T., Teng, P., and Metselaar, K. (Eds.), Systems Approaches for Agricultural Development, Vol. 2. Kluwer Academic Publishers, Dordrecht, The Netherlands. pp. 233-252.
Kidson, J.W., Thompson, C.S., 1998. Comparison of statistical and model-based downscaling techniques for estimating local climate variations. J. Climate 11, 735-753.
Lall, U., Sharma, A., 1996. A nearest neighbor bootstrap for time series resampling. Water Resour. Res. 32, 679-693.
Latif, M., Anderson, D., Barnett, T., Cane, M., Kleeman, R., Leetmaa, A., O'Brien, J., Rosati, A., Schneider, E., 1998. A review of the predictability and prediction of ENSO. J. Geophys. Res. 103, 14,375-14,393.
Mason, S. J., Goddard, L., Graham, N. E., Yulaeva, E., Sun, L., Arkin, P. A., 1999. The IRI seasonal climate prediction system and the 1997/98 El Niño event. Bull. Amer. Meteorol. Soc. 80, 1853-1873.
Mavromatis, T., Jones, P.D., 1998. Comparison of climate change scenario construction methodologies for impact assessment studies. Agric. Forest Meteorol. 91, 51-67.
Mavromatis, T., Hansen, J.W., 2001. Interannual variability characteristics and simulated crop response of four stochastic weather generators. Agric. For. Meteorol. 109, 283-296.
Mearns, L.O., Giorgi, F., McDaniel, L., Shields, C., 1995. Analysis of daily variability of precipitation in a nested regional climate model: comparison with observations and doubled CO2 results. Global and Planetary Change 10, 55-78.
Mearns, L.O., Rosenzweig, C., Goldberg, R., 1996. The effects of changes in daily and interannual climatic variability on CERES-Wheat: a sensitivity study. Climatic Change 32, 257-292.
Meinke, H., Stone, R.C., Hammer, G.L., 1996. SOI phases and climate risk to peanut production: a case study for Northern Australia. International Journal of Climatology 16, 783-789.
Mutai, C.C., Ward, M.N., Coleman, A.W., 1998. Towards the prediction of the East Africa short rains based on sea-surface temperature-atmosphere coupling. Int. J. Climatol., 18, 975-997.
Ngugi, R.K., 2002. Climate Forecast Information: The Status, Needs and Expectations among Smallholder Agro-pastoralists in Machakos District, Kenya. IRI Technical Report 02-04. International Research Institute for Climate Prediction, Palisades, New York.
Ogallo, L.J., Janowiak, J.E., Halpert, M.S., 1988. Teleconnection between seasonal rainfall over East Africa and global seas surface temperature anomalies. J. Met. Soc. Japan 66, 807-822.
Palmer, T.N., Anderson, D.L.T., 1994. The prospects for seasonal forecasting. Quart. J. Roy. Meteor. Soc. 120, 755-793.
Pickering, N.B., Hansen, J.W., Jones, J.W., Wells, C.M., Chan, V.K., Godwin, D.C., 1994. WeatherMan: a utility for managing and generating daily weather data. Agronomy Journal 86, 332-337.
Probert, M.E. (Ed.), 1992. A Search for Strategies for Sustainable Dryland Cropping in Semi-arid Eastern Kenya. ACIAR Proceedings No. 41. Australian Centre for International Agricultural Research, Canberra, Australia.
Probert, M.E., Keating, B.A., Siambi, M.N., Okalebo,

J.R., 1994. Management of soil fertility in climatically risky environments. In: Craswell, E.T., Simpson, J. (Eds.) Soil Fertility and Climatic Constraints in Dryland Agriculture. ACIAR Proceedings No. 54. Australian Centre for International Agricultural Research, Canberra, Australia. pp. 51-63.

Probert, M.E., Keating, B.A., Larkens, A.G., Siambi, M.N., 2001. Regional assessment of strategies for maize production in semi-arid eastern Kenya. Tropical Agriculture Technical Memorandum No. 8. CSIRO Tropical Agriculture, Indooroopilly, Australia. 34 pp.

Richardson, C.W., 1985. Weather simulation for crop management models. Trans. ASAE 28, 1602-1606.

Riha, S.J., Wilks, D.S., Simeons, P., 1996. Impacts of temperature and precipitation variability on crop model predictions. Climatic Change 32, 293-311.

Ritchie, J.T., Singh, U., Godwin, D.C., Bowen, W.T., 1998. Cereal growth, development and yield. In: Tsuji, G.Y., Hoogenboom, G., Thornton, P.K. (Eds.), Understanding Options for Agricultural Production. Kluwer Academic Publishers, Dordrecht, The Netherlands, pp. 79-98.

Roeckner, E., Oberhuber, J.M., Bacher, A., Christoph, M., Kirchner, I., 1996. ENSO variability and atmospheric response in a global coupled atmosphere-ocean GCM. Climate Dynamics 12, 737-754.

Ropelewski, C. F., Halpert, M., 1987. Global and regional scale precipitation patterns associated with the El Niño/Southern Oscillation. Monthly Weather Review 115, 1606-1626.

Rosenzweig, C. 1994. Maize suffers a sea-change. Nature 370, 175-176.

Royce, F.S., Jones, J.W., Hansen, J.W., 2001. Model-based optimization of crop management for climate forecast applications. Transactions of the American Society of Agricultural Engineers 44, 1319-1327.

Semenov, M.A., Porter, J.R., 1995. Climatic variability and the modelling of crop yields. Agric. Forest Meteorol. 73, 265-283.

Solman S, Nuñez, M., 1999. Local estimates of global climate change: A statistical downscaling approach. Int. J. Climatology. 19, 835-861.

Stern, R.D., Coe, R., 1984. A model fitting analysis of daily rainfall data. Journal of the Royal Statistical Society A147, 1-34.

Stone, M., 1974. Cross-validatory choice and assessment of statistical predictions (with discussion). Journal of the Royal Statistical Society B 36, 111-147.

Stone, R., Smith, I., McIntosh, P., 2000. Statistical methods for deriving seasonal climate forecasts from GCM's. In: Hammer, G.L., Nicholls, N., Mitchell, C. (Eds.), Applications of Seasonal Climate Forecasting in Agricultural and Natural Ecosystems. Kluwer, Dordrecht, The Netherlands, pp. 135-147.

Trenberth, K., 1997. The definition of El Niño. Bull. Amer. Meteor. Soc. 78, 2771-2777.

Vaux, H.J. Jr., Pruitt, W.O., 1983. Crop-water Production Functions. In: Advances in Irrigation, Volume 2. Academic Press, New York. pp. 72-79.

Wilks, D.S., 1999. Interannual variability and extreme-value characteristics of several stochastic daily precipitation models. Agric. For. Meteorol. 93, 153-169.

Wilks, D.S., 2002. Realizations of daily weather in forecast seasonal climate. J. Hydrometeorology 3, 195-207.

Wilby, R.L., Dawsonb, C.W., Barrow, E.M., 2002. SDSM – a decision support tool for the assessment of regional climate change impacts. Environmental Modelling & Software 17, 145-157.

Willmott, C.J., 1981. On the validation of models. Phys. Geogr. 2, 184-194.

Willmott, C.J., 1982. Some comments on the evaluation of model performance. Bul. Amer. Meteorol. Soc. 63, 1309-1313.

Woolhiser, D.A., Roldán, J., 1982. Stochastic daily precipitation models. 2. A comparison of distributions of amounts. Water Resour. Res. 18, 1461-1468.

Woolhiser, D.A., Keefer, T.O., Redmond, K.T., 1993. Southern Oscillation effects on daily precipitation in the southwestern United States. Water Resour. Res. 29, 1287-1295.

Zorita, E., von Storch, H., 1999. The analog method as a simple statistical downscaling technique: comparison with more complicated methods. J. Climate 12, 2474-2489.

Table 1. Summary descriptions of maize prediction scenarios.

Scenario	Description
1. Baseline (observed rainfall)	Yields simulated with observed daily weather data. This scenario serves as a baseline for evaluating the other scenarios.
2. Nonlinear regression	Yields predicted by regression from the first two PCs from the MOS correction of seasonal (Oct-Dec) GCM output fields.
3a. *k* nearest neighbor, 1 PC	Yields predicted by *k* nearest neighbor weighted average from analog years, based on the first PC of MOS-corrected seasonal (Oct-Dec) GCM fields.
3b. *k* nearest neighbor, 2 PCs	Yields predicted by *k* nearest neighbor weighted average from analog years, based on the first two PCs of MOS-corrected seasonal (Oct-Dec) GCM fields.
4a. Stochastic disaggregation	Yields simulated with 30 years of stochastic daily weather disaggregated from monthly (Oct-Jan) rainfall totals derived from ensemble mean GCM predictors.
4b. Stochastic disaggregation wth π	Yields simulated with 30 years of stochastic daily weather disaggregated from monthly (Oct-Jan) rainfall totals, and π, derived from ensemble mean GCM predictors.

Table 2. Goodness of fit statistics, observed and cross-validated hindcast total rainfall, relative frequency and mean wet-day intensity.

Period	*RMSE*	*MBE*	*r*	*d*
	Total rainfall (mm)			
October-December	129.9	1.7	0.604 ***	0.733
September	9.6	0.0	0.154 n.s.	0.295
October	40.7	0.6	0.532 ***	0.683
November	87.4	-0.1	0.560 ***	0.704
December	56.6	0.2	0.408 *	0.563
January	65.1	-0.1	0.365 *	0.523
	Relative frequency			
October-December	0.083	0.000	0.750 ***	0.848
September	0.063	0.000	0.203 n.s.	0.392
October	0.110	0.000	0.644 ***	0.765
November	0.130	0.001	0.560 ***	0.697
December	0.170	-0.010	0.493 **	0.639
January	0.184	-0.002	0.118 n.s.	0.352
	Mean intensity (mm d^{-1})			
October-December	3.01	0.13	0.146 n.s.	0.305

Table 3. Goodness-of-fit statistics for maize yield predictions.

	RMSE	***MBE***	***r***	***d***
Scenario	**(Mg ha^{-1})**			
2. Nonlinear regression	0.962	-0.006	0.571	0.719
3a. *k* nearest neighbor, 1 PC	0.998	-0.024	0.527	0.702
3b. *k* nearest neighbor, 2 PCs	0.984	0.017	0.531	0.680
4a. Stochastic disaggregation	1.164	0.599	0.575	0.720
4b. Stochastic disaggregation with π	1.195	0.626	0.545	0.696

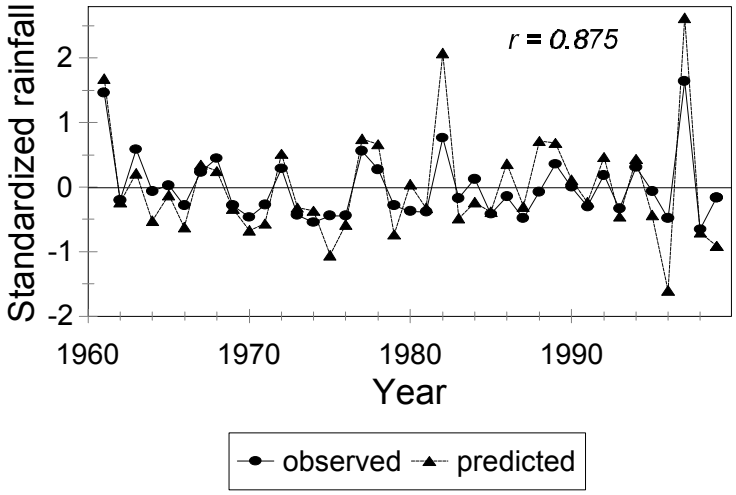

Figure 1. Standardized values of observed October-December rainfall averaged for 52 stations in Kenya, and ECHAM4.5 global climate model rainfall (mean of 24 ensembles) averaged between 33°-43°E and 6°S-6°N.

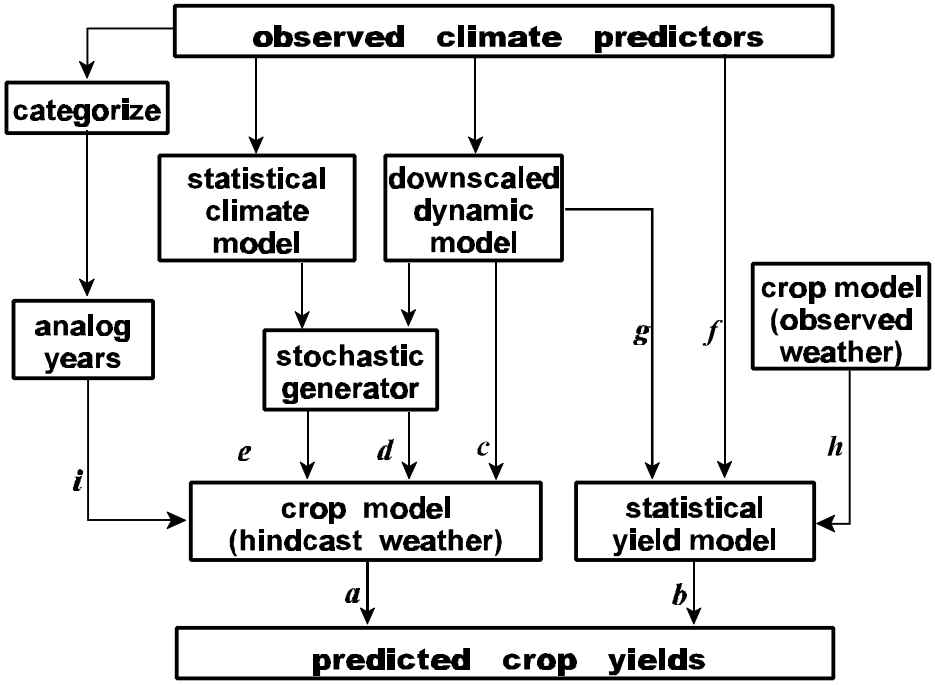

Figure 2. Potential information pathways from large-scale observed climatic predictors to simulation-based predicted crop yields.

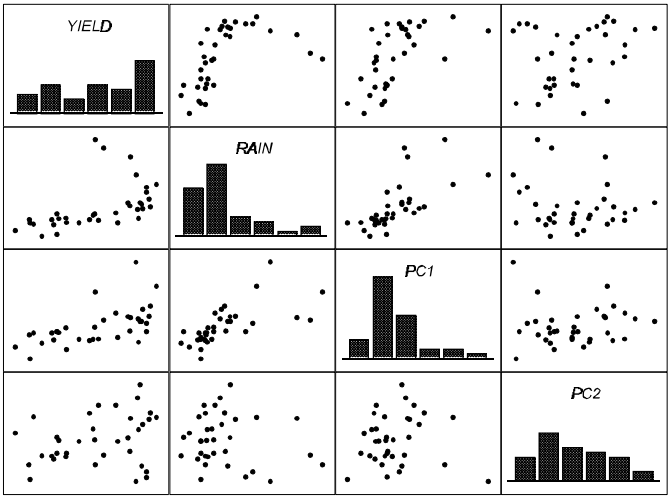

Figure 3. Histograms and scatter plots of simulated maize yields, October-December rain, and the first two principle components (*PC1* and *PC2*) of ECHAM 4.5 output fields for October-December.

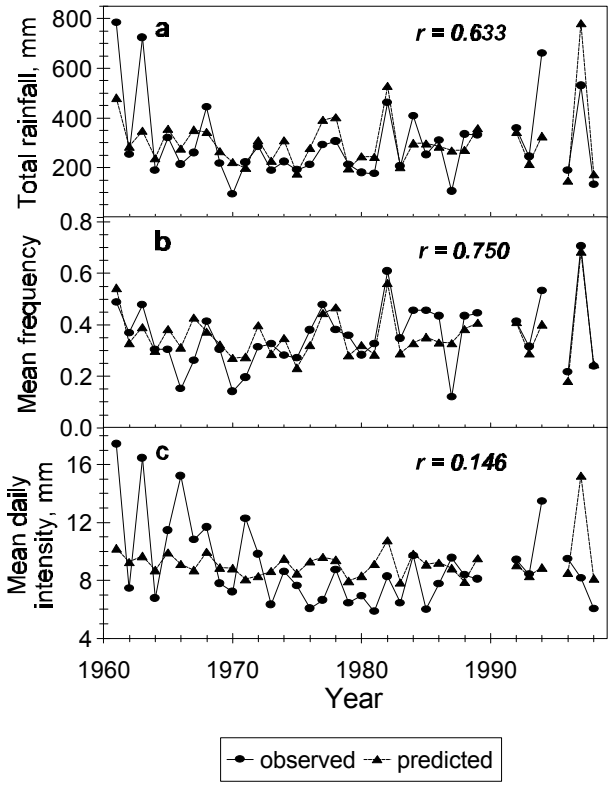

Figure 4. Total rainfall (a), mean wet-day frequency (b) and mean daily intensity (c) of October-December rainfall observed and hindcast from transformed ECHAM 4.5 output fields.

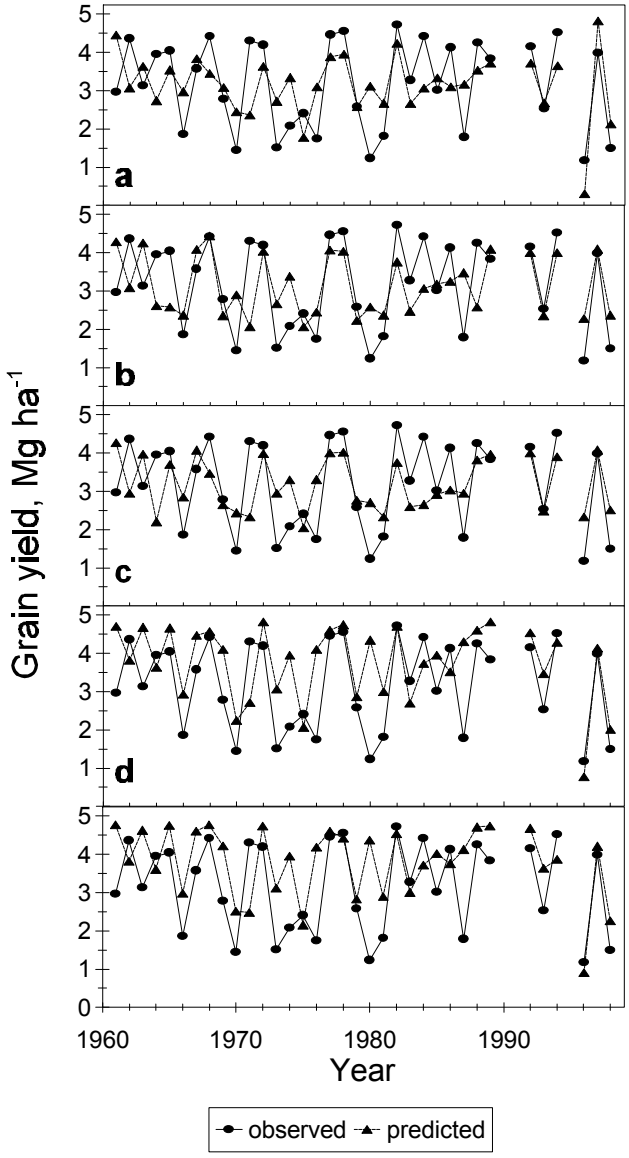

Figure 5. Maize yields simulated from observed weather, and hindcast by nonlinear regression (a), *k* nearest neighbors using 1 (b) and 2 PCs (c), and stochastic disaggregation from hindcast monthly rainfall totals alone (d) and monthly rainfall totals plus hindcast wet-day probability (e).

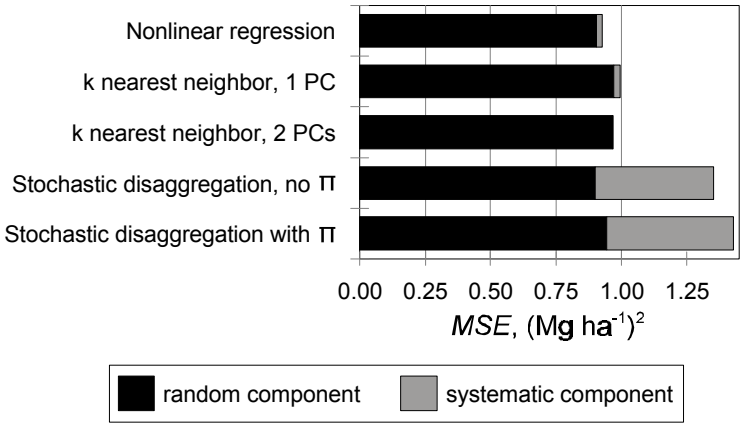

Figure 6. Mean squared error of prediction (*MSE*) of maize yield hindcast scenarios, and its random and systematic components.

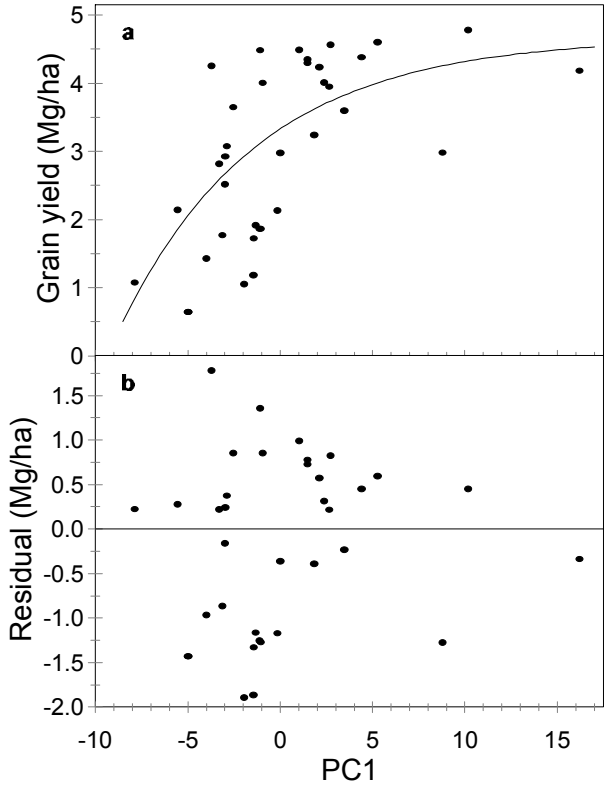

Figure 7. Simulated maize yields and the best-fit regression curve, $\hat{y} = 3.330 + 1.344\left(1 - \exp\left(-0.3316\ PC1\right)\right)$ (a), and regression residuals (b).

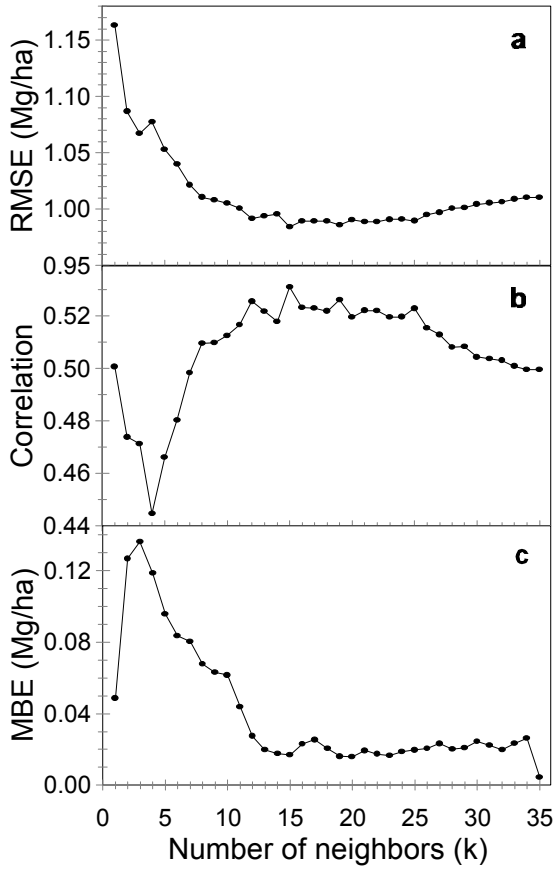

Figure 8. Sensitivity of *RMSE* (a), correlation (b) and *MBE* (c) of maize yield predictions, based on the *k*-nearest neighbor method, to the number of neighbors, *k*.